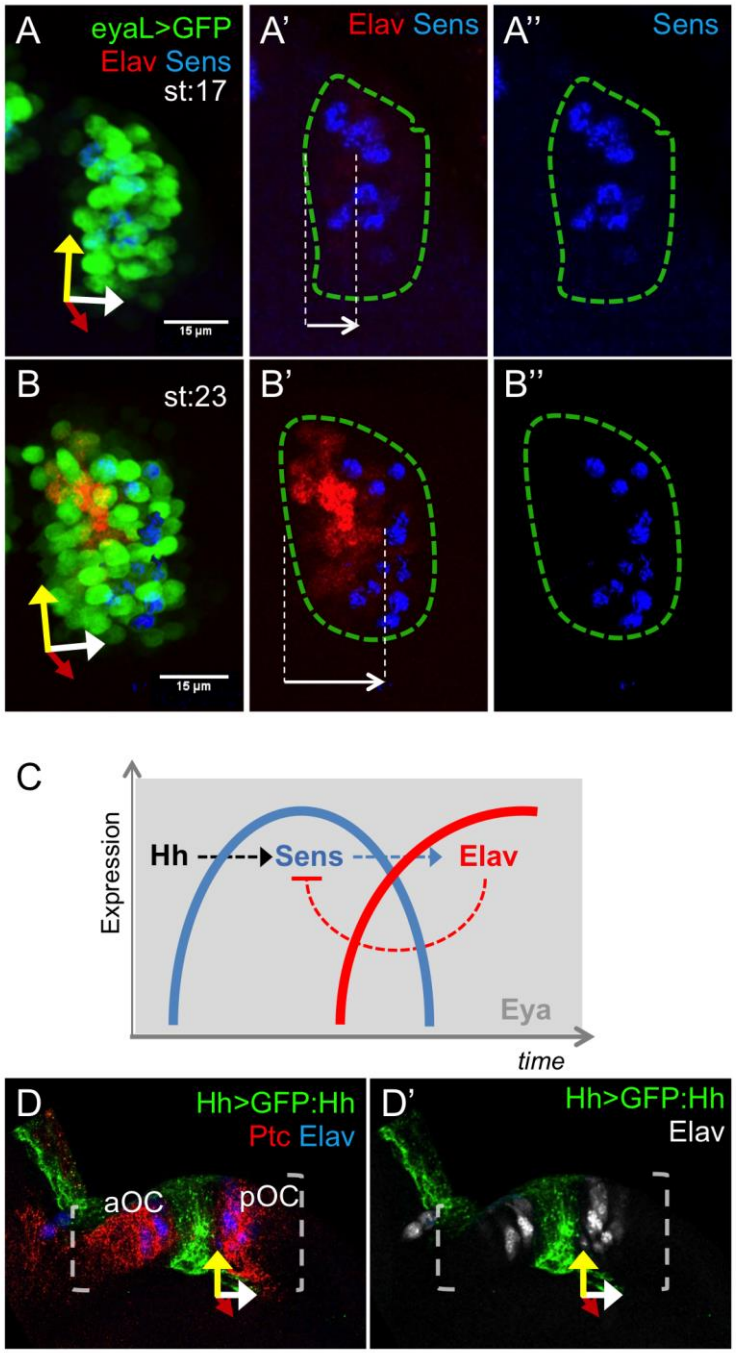

Figure S1. **R cells do not express Hh and differentiate following a *senseless-Elav* sequence**. (A,B) Sens and Elav mark the progress from precursors (Sens, red) to differentiating photoreceptors (Elav, blue). Confocal image of a posterior ocellar region of third instar stage 17 ommatidia (A) and 23 ommatidia (B) discs of an *eya>GFP* larvae. Eya (green) expression marks the ocellar competent region (outlined

in A'-A'' and B'-B''). At St17 Sens is expressed adjacent or close to the proximal border of the ocellus and no Elav R cells have yet differentiated. At St23, Elav R cells have differentiated and new Sens-positive cells are induced distal to them. The white arrows in A' and B' indicate the position of the Sens front relative to the Hh source. Axes as in Figure 1. (C) Schematic representation of the temporal changes in gene expression experienced by any cell in the ocellar complex. Competent cells (expressing Eya), upon receiving Hh signal, progress along their differentiation program, expressing Sens first, then Elav. The connecting links are dashed to indicate that the activations (arrow) or repression (flat end) are likely indirect. (D,D') Confocal image of an ocellar region (bracketed) from a *hh-Gal4>UAS-GFP:Hh* disc, stained for GFP, Ptc and Elav (D). (D') shows the GFP and Elav channels only. Elav-expressing R cells, which differentiate in a region of Hh signaling (i.e. Ptc-expressing), do not transcribe Hh.

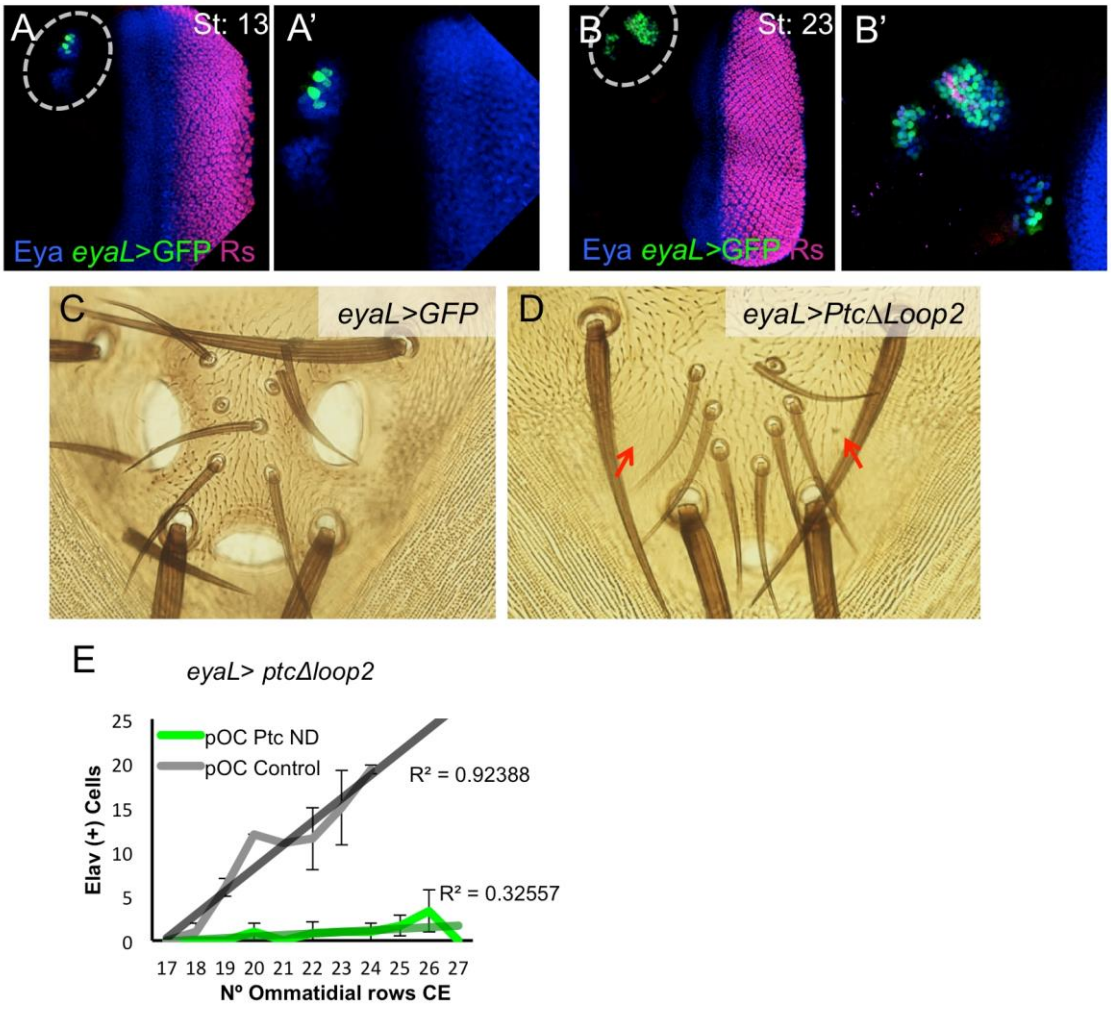

Figure S2. Driving a dominant-negative *Ptc* in the ocelli using the *eyaL-GAL4* blocks ocellar development. (A,B) Enhancer activity of the FlyLight R20D09 GAL4 driver line ("eyaL-GAL4") before (A: stage 13; A':close-up) and after (B: stage 23; B':close-up) R cell differentiation onset. Discs of eyaL-GAL4; UAS-GFP (*eyaL>GFP*) larvae were stained for Eya, GFP and Elav (R cells). Ocellar region is enclosed in the dashed oval. In (A), GFP signal is activated in the Eya-expressing ocellar domains. In later stages (B) GFP signal overlaps Eya. Therefore, EyaL-GAL4 drives expression in the ocellar *eya* domains exclusively. (C,D) Ocellar regions of adult flies. Control (C: *eyaL-GAL4; UAS-GFP*, "eyaL>GFP") and *eyaL-GAL4; UAS-ptcΔloop2* (D: "eyaL>ptcΔloop2"). PtcΔloop2 acts as a Hh-dominant negative protein (see Material and Methods and references). In *eyaL>ptcΔloop2* flies the ocelli are severely

reduced or absent (red arrows). (E) Dynamics of R cells differentiation in the posterior ocellus (pOC) (as Elav-expressing cells) in *eyaL>GFP* (“control”) and *eyal>ptcΔloop2* (“ptcDN”), with linear fits and R^2 values.

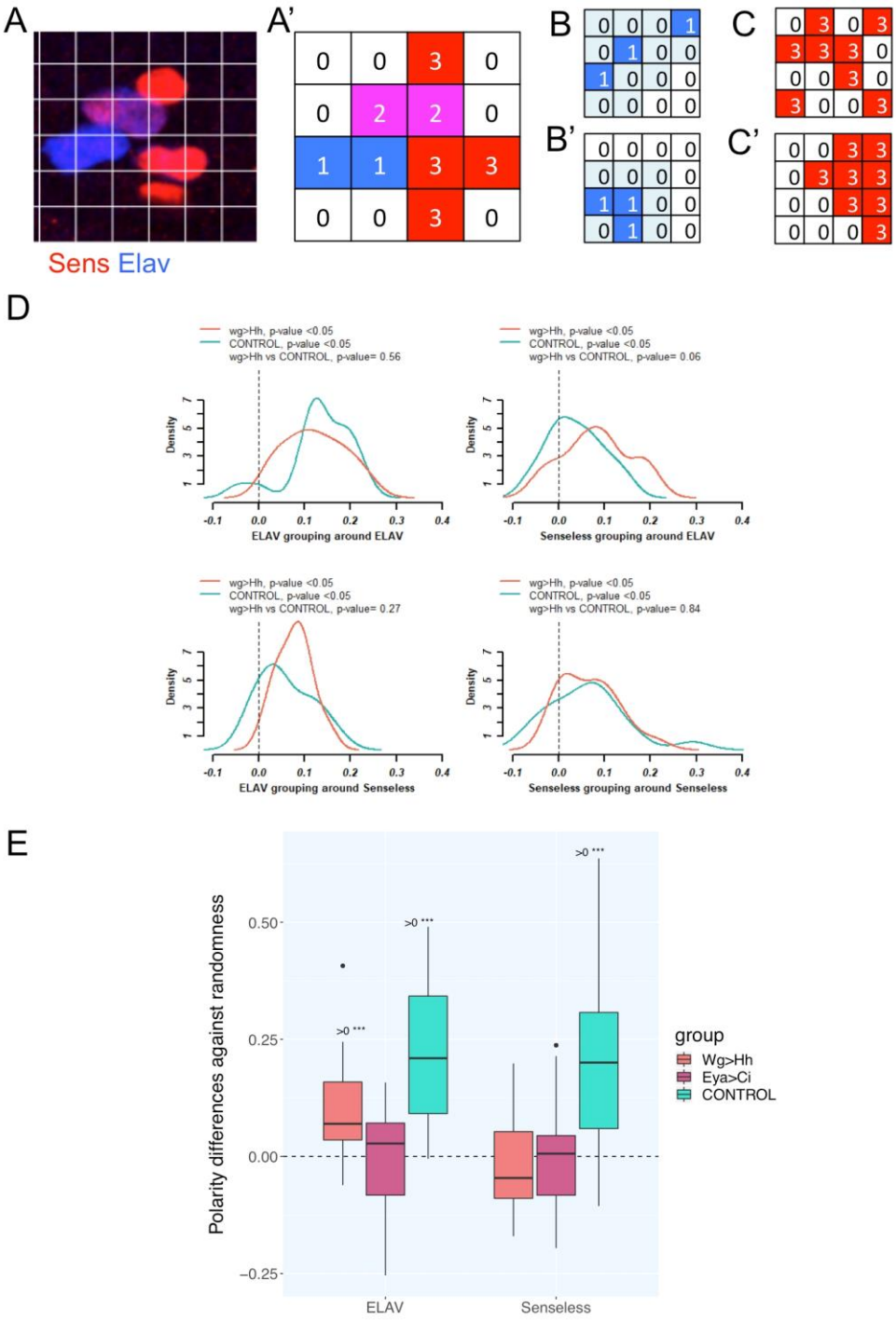

Figure S3. Statistical analysis of Sens/Elav pattern in control, *wg>Hh* and *eyaL>Ci-PKA* ocelli. (A) Image of a Sens and Elav staining with superimposed grid and its translation into a bidimensional matrix (A'), in which the three different states detected, Elav+Sens-, Elav(+)Sens(+) and Elav-Sens+ are coded as 1, 2 and 3, respectively. (B-C') Examples illustrating the two statistics used to analyze the pattern of Sens and Elav expression. (B,B') Example of "random" (B) and "grouped" (B') "1"

matrix. Neighbors are marked in light colors. From left to right and from top to bottom, the neighbor proportion is 0, 1/8 and 1/5, 0.1 on average for (B), and 2/5, 2/8 and 2/5, 0.4 on average for (B'). (C,C') Example of "non-polarized" (C) and "polarized" (C') "3" matrix. Polarity is calculated as the probability of finding a "3" in the last column, estimated using column number as predictor, minus the expected probability of success in the whole matrix (8/16). Polarity will be close to 0 for (C, "non-polarized") and significantly larger than 0 for (C', "polarized"). See methods and Results for further details. (D) Represents the departure from random grouping of different cell states ("order"). Both, control and *wg>Hh* patterns show significant ordered grouping for all four comparisons ($p<0.05$), although they do not differ significantly among them. "Density" refers to the density function, generated from the data histogram as a smoothened curve. (E) When the ordered distribution of Elav or Sens along the proximodistal axis ("polarity") is computed, the pattern in control ocelli is significantly polarized and much more so than in *wg>Hh* samples. This is also the case of *eyaL>Ci-PKA* samples. "0>***" refers to those groups in which their polarity were significantly higher than 0 ($p<0.05$). Only posterior ocelli were analyzed.

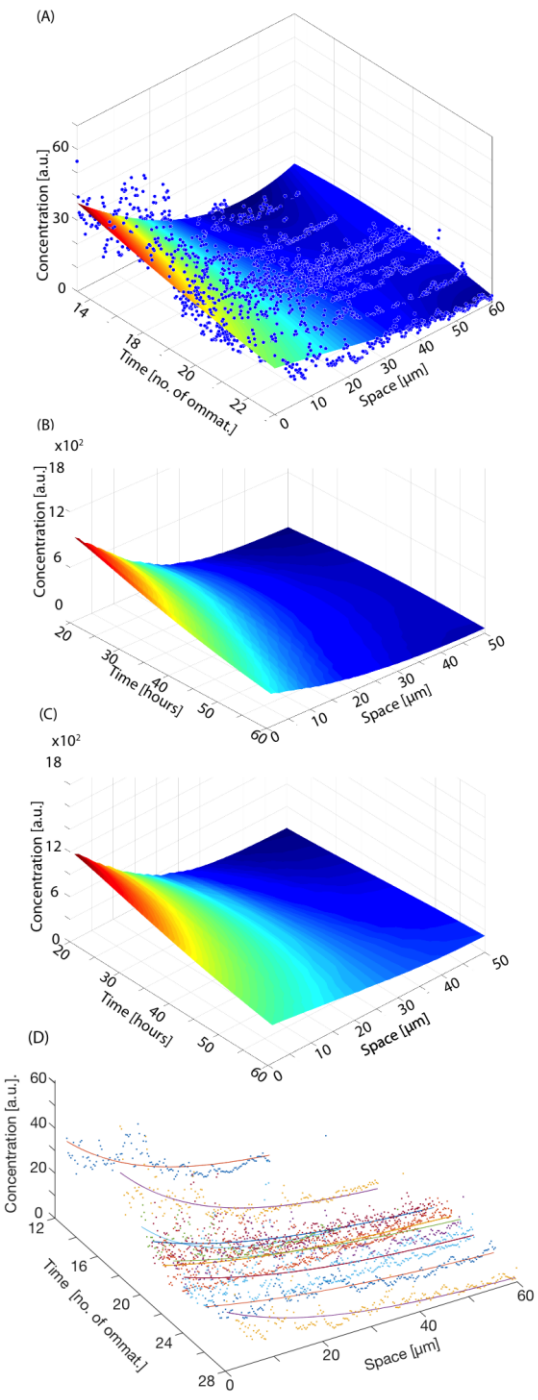

Figure S4. Hh gradient dynamics. (A) Plot of Hh:GFP signal (“concentration” in arbitrary units [a.u.]) as a function of time and space (in µm), obtained from fixed samples at specific developmental time points (as no. of ommatidia in the compound eye). Model parameters were constrained using this data. (B,C) Plots of Hh dynamics from the simulations, not

including (B) or including (C) the attenuation of Ptc expression in differentiating R cells. Note that in (C) (but not in (B)) the Hh gradient spreads farther with time, as observed in the measured profiles (A). (D) Exponential fitting (lines) of the spatial distribution of the Hh concentration profiles in (A).

Table S1. Values, units and sources of model parameters

Variable	value	Units	Source
Dimensions of Ocelus	55 x 55	μm^2	Experim. estimated
Number of cells in Ocelus	110	-	Experim. estimated
Number of cells in row	10	-	Experim. estimated
Number of rows	11	-	Experim. estimated
Total Time	50	hours	Experim. estimated
Rate of Hh expression 1	200		
High Rate of Hh expression	440		
k_{Hh}	0.002	1/hour	Value that best fits the experimental data
α	20	1/hour	fitted
β	10	1/hour	fitted
A	20	adimensional	fitted
B	1	adimensional	fitted
C	40		
m	3	adimensional	fitted
D	4	μm^2/hour	Value that best fits the experimental data.
Theshold for Elav	40		

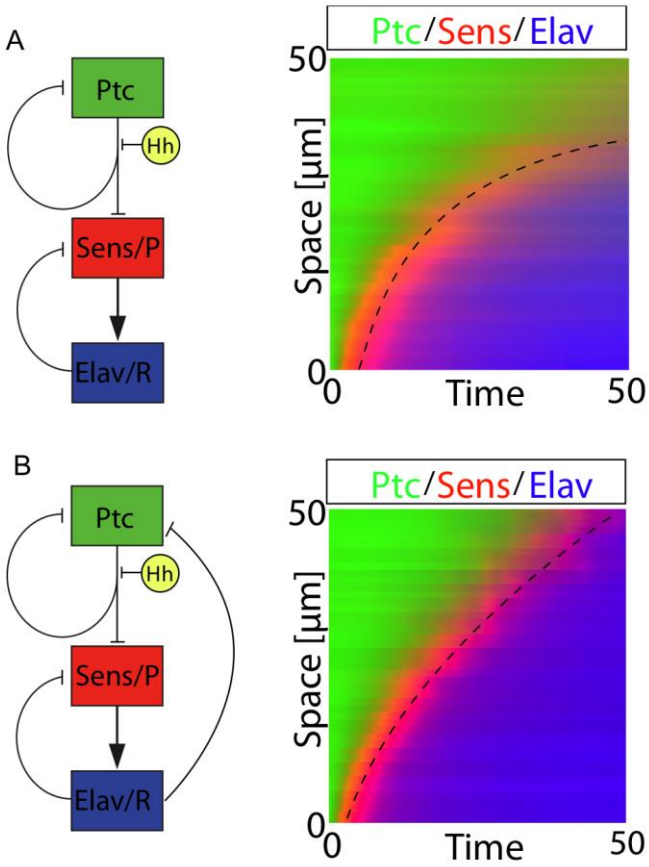

Figure S5. Differentiation dynamics and Ptc attenuation with a constant Hh production rate. Cartoon diagrams of the model for the Hh signaling pathway without considering (A) or considering (B) a negative feedback from Elav-expressing R cells to Ptc and its downstream effects (left), and corresponding spatio-temporal dynamics (right). In (A) R cells (blue) accumulate hyperbolically and do not reach the end of the competent region within the time frame of 50h. In (B) (with negative feedback, all other parameters being the same) R accumulation dynamics is close to linear and R differentiation reaches the end of the competent region. Simulations performed maintaining a constant Hh production rate.

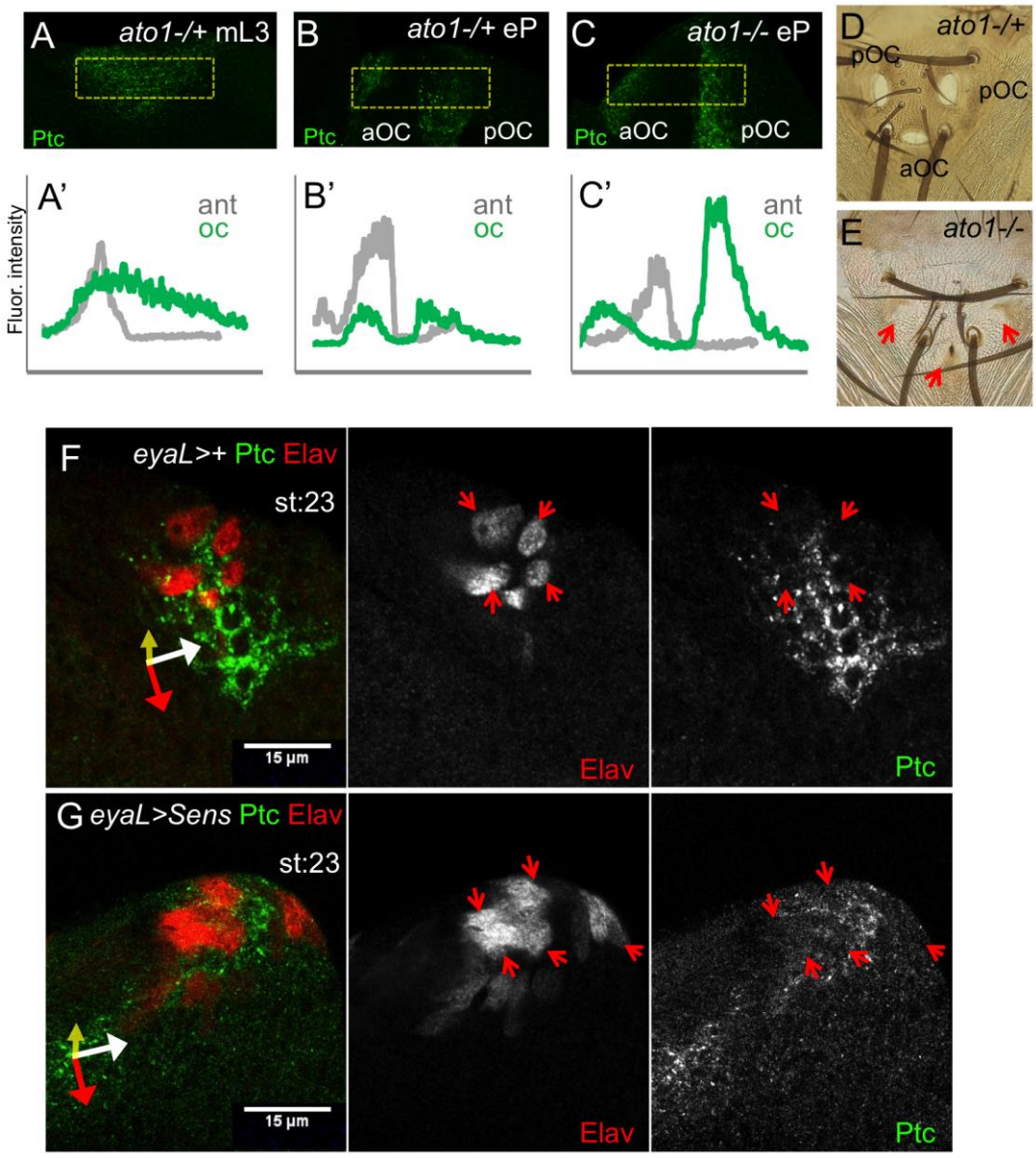

Figure S6. Ptc signal and R cell differentiation. (A-C) Ptc signal in the ocellar regions of mid L3 (mL3; A) and early pupa (eP; B) *ato1*+/- discs, and eP of an *ato1-/-* disc (C). (A'-C') Overlapped spatial expression profiles of Ptc signal in the ocellar regions ("oc", green) and in the antenna of the same disc ("ant", grey), this latter used as an internal normalization. In *ato1-/+* controls, the maximal ocellar Ptc signal is similar to that of the antenna (A'; n=6) in early discs but drops in later stages (early pupa: B', n=5). However, in late stage *ato1-/-* the Ptc signal ratio remains high (C'; n=6). Posterior and anterior ocelli (pOC and aOC) are marked in (B,C). In (A) the split

of the Ptc domain in the two ocellar primordia has not yet occurred. (D,E) Adult ocellar complexes of *ato1+/- and ato1-/-* flies. In homozygous *ato1* individuals ocelli fail to develop. (F,G) Control (F: *eyaL*>+) and Sens-expressing (G: *eyaL*>*Sens*) pOC at st:23 stained for Elav and Ptc. In *eyaL*>*Sens* there is an increase in the number of Elav cells. Ptc signal is reduced in all Elav cells and, as a consequence, in *eyaL*>*Sens* Ptc levels are globally reduced also. Red arrows point to Elav cells.

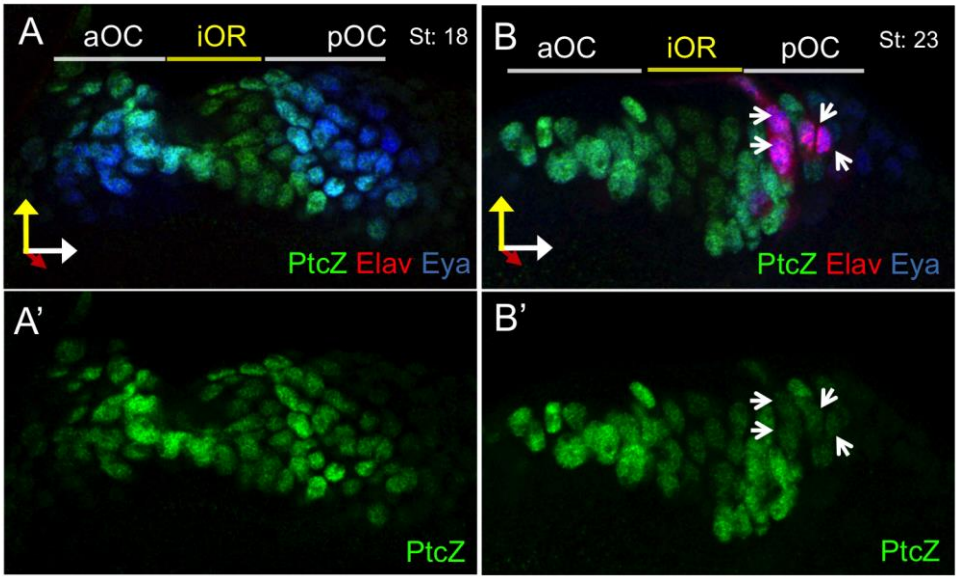

Figure S7. Expression of a *ptc* transcriptional reporter (ptc-Z) is down regulated in differentiating photoreceptors. Ocellar complex region of *ptc-Z* discs stained for β-galactosidase (PtcZ), Elav and Eya (A,B). PtcZ channel alone is shown in (A',B'). St 18 ocellar complex region, prior to the initiation of R cell differentiation. (B,B') St 23 ocellar complex region. Arrows point to Elav-expressing R cells. The anterior (aOC) and posterior (pOC) ocellar retinas as well as the interocellar region (iOR) are marked. PtcZ signal in the iOR is detected, although weak, likely due to β-galactosidase perdurance.

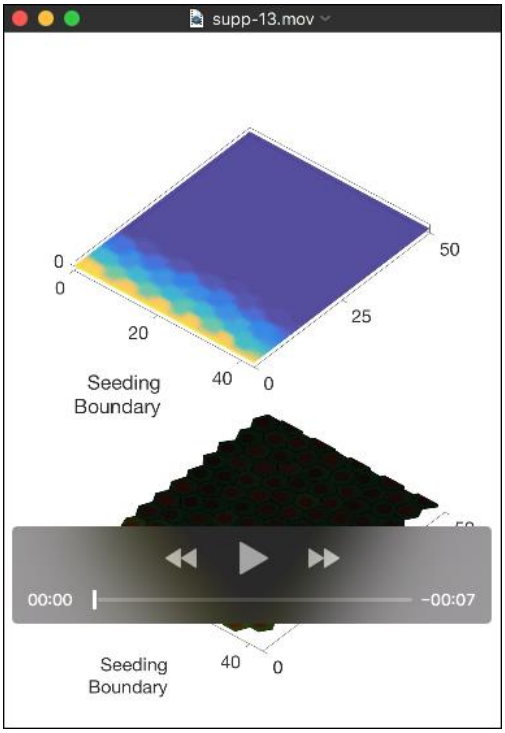

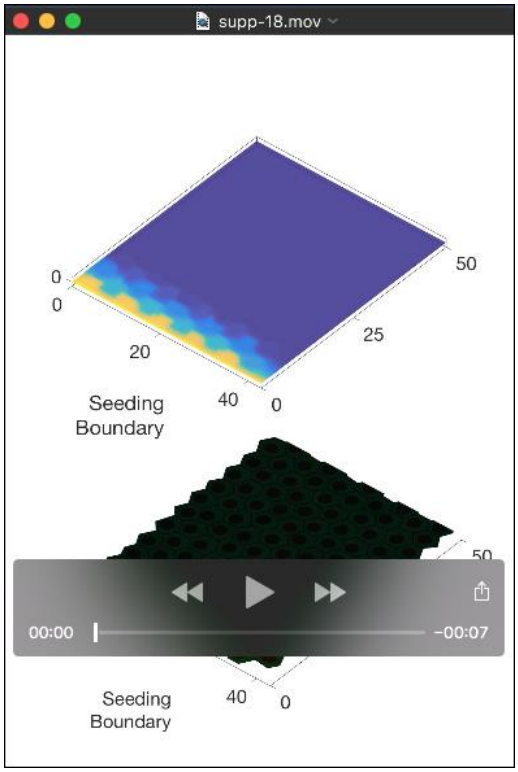

Movies 1 and 2. Time-lapse movies of the simulation without (Movie 1) and with (Movie 2) Ptc negative feedback regulation.

Upper panel shown the concentration of Hh across the domain. Lower panel shows the cellular concentration of Ptc (green), Sens (red) and Elav (blue). Despite the

variable response to Hh due to cell variability, a wave in photoreceptor differentiation (blue cells) can be observed as traveling away from the Hh source. The first movie (no Ptc downregulation) shows that the wave velocity diminishes and stops before reaching the end of the domain. The Hh gradient does not flatten. The second movie includes Ptc negative feedback, and shows how the differentiation wave moves at constant speed and reaches the end of the domain. The Hh gradient flattens.

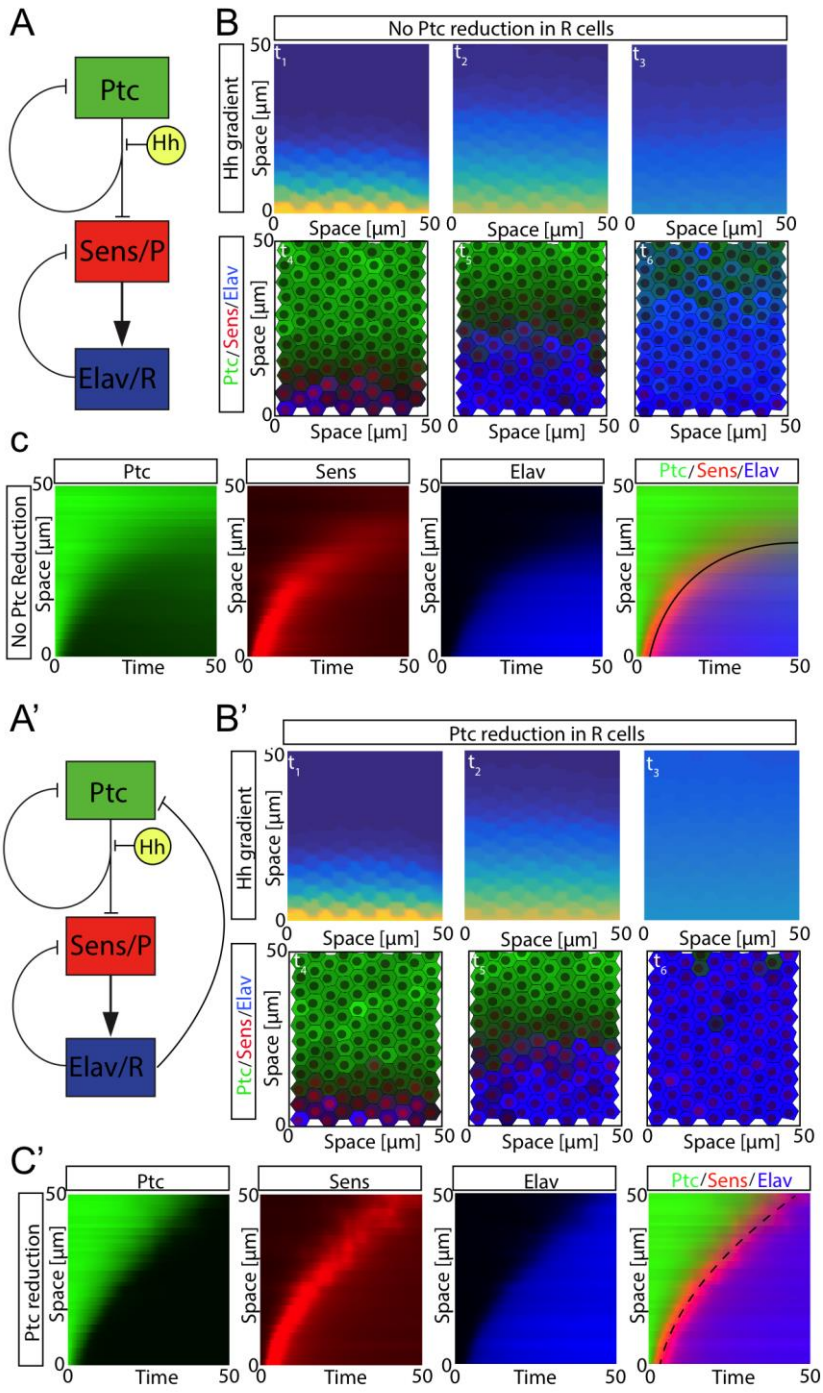

Figure S8. Dynamics of Hh signaling in response to its gradient. (A,A') Shape of the interactions taken into account in the model. (B,B') Snapshots of the simulation at different times. Images above depict the Hh profile, while the bottom images represent the cell differentiation state. Red: Sens cells; Blue: Elav R cells; Green: free Ptc (See supp. videos 1 and 2). (C,C') Space-time plots of free Ptc (green),

Sens (red) and Elav (blue) and superposition of the three across the ocellus. The black lines (solid in (C) and dashed in (C')) are used as a guide to the eye to show the speed of the differentiation wave.

The source code file can be downloaded here